ESC European Society of Cardiology

Cardiovascular Research (2017) **113**, 1338–1350
doi:10.1093/cvr/cvx118

Exosomes secreted by cardiomyocytes subjected to ischaemia promote cardiac angiogenesis

Teresa M. Ribeiro-Rodrigues[1,2], Tiago L. Laundos[3,4,5], Rita Pereira-Carvalho[1,2], Daniela Batista-Almeida[1,2], Ricardo Pereira[1,2], Vanessa Coelho-Santos[1,2,6], Ana P. Silva[1,2,6], Rosa Fernandes[1,2], Monica Zuzarte[1,2], Francisco J. Enguita[7], Marina C. Costa[7], Perpetua Pinto-do-Ó[3,4,5], Marta T. Pinto[3,8], Pedro Gouveia[2,9], Lino Ferreira[2,9], Justin C. Mason[10], Paulo Pereira[1,2,11], Brenda R. Kwak[12], Diana S. Nascimento[3,4], and Henrique Girão[1,2]*

[1]Institute for Biomedical Imaging and Life Sciences (IBILI), University of Coimbra, Azinhaga de Sta Comba, 3000-354 Coimbra, Portugal; [2]CNC.IBILI, University of Coimbra, Portugal; [3]Instituto de Investigação e Inovação em Saúde (i3S), Universidade do Porto, Porto, Portugal; [4]INEB–Instituto Nacional de Engenharia Biomédica, Universidade do Porto, Porto, Portugal; [5]Instituto de Ciências Biomédicas Abel Salazar (ICBAS), Universidade do Porto, Porto, Portugal; [6]Institute of Pharmacology and Experimental Therapeutics, University of Coimbra, Azinhaga de Sta Comba, 3000-354 Coimbra, Portugal; [7]Instituto de Medicina Molecular, Faculty of Medicine, University of Lisbon, 1649-028 Lisboa, Portugal; [8]Institute of Molecular Pathology and Immunology (Ipatimup), University of Porto, Portugal; [9]CNC-Center for Neurosciences and Cell Biology, University of Coimbra, 3000 Coimbra, Portugal; [10]Vascular Sciences Unit, Imperial Centre for Translational & Experimental Medicine, Imperial College London, London, UK; [11]CEDOC, NOVA Medical School, NOVA University of Lisbon, Lisboa 1169-056, Portugal; and [12]Department of Pathology and Immunology, and Department of Medical Specialties–Cardiology, University of Geneva, CH-1211 Geneva, Switzerland

Received 19 December 2016; revised 19 April 2017; editorial decision 26 May 2017; accepted 15 June 2017; online publish-ahead-of-print 19 June 2017

Time for primary review: 60 days

Aims Myocardial infarction (MI) is the leading cause of morbidity and mortality worldwide and results from an obstruction in the blood supply to a region of the heart. In an attempt to replenish oxygen and nutrients to the deprived area, affected cells release signals to promote the development of new vessels and confer protection against MI. However, the mechanisms underlying the growth of new vessels in an ischaemic scenario remain poorly understood. Here, we show that cardiomyocytes subjected to ischaemia release exosomes that elicit an angiogenic response of endothelial cells (ECs).

Methods and results Exosomes secreted by H9c2 myocardial cells and primary cardiomyocytes, cultured either in control or ischaemic conditions were isolated and added to ECs. We show that ischaemic exosomes, in comparison with control exosomes, confer protection against oxidative-induced lesion, promote proliferation, and sprouting of ECs, stimulate the formation of capillary-like structures and strengthen adhesion complexes and barrier properties. Moreover, ischaemic exosomes display higher levels of metalloproteases (MMP) and promote the secretion of MMP by ECs. We demonstrate that miR-222 and miR-143, the relatively most abundant miRs in ischaemic exosomes, partially recapitulate the angiogenic effect of exosomes. Additionally, we show that ischaemic exosomes stimulate the formation of new functional vessels *in vivo* using *in ovo* and Matrigel plug assays. Finally, we demonstrate that intramyocardial delivery of ischaemic exosomes improves neovascularization following MI.

Conclusions This study establishes that exosomes secreted by cardiomyocytes under ischaemic conditions promote heart angiogenesis, which may pave the way towards the development of add-on therapies to enhance myocardial blood supply.

Keywords Extracellular vesicles • Exosomes • Ischaemia • Angiogenesis • Myocardial infarction • Coronary collateral circulation

* Corresponding author. Tel: +351239480221; fax: +351239480217, E-mail: hmgirao@fmed.uc.pt

1. Introduction

Myocardial infarction (MI), the leading cause of morbidity and mortality worldwide,[1] occurs when blood supply to a certain region of the heart is totally or partially blocked, with the consequent shortage of oxygen and nutrients supply to cardiac cells, a process called heart ischaemia. In order to ensure the proper replenishment of blood to the deprived areas, affected cells release signals, including growth factors, which stimulate the growth of new vessels. For example, a moderate chronic occlusion of coronaries can result in the development of coronary collateral circulation (CCC), as part of a compensatory strategy to ensure a sufficient blood supply to the ischaemic region.[2,3] Also healthy physiological cardiac hypertrophy, usually associated with physical exercise, requires an adequate vascular growth that accompanies myocytes enlargement.[4] Although inflammatory mediators and growth factors, such as VEGF and b-FGF, have been implicated in the formation of new vessels in the heart, the biological processes involved in the stimuli-induced angiogenesis remain largely unknown.[3] Angiogenesis, which is the formation of new blood vessels formation from pre-existing vasculature, is a highly controlled mechanism that involves the local breakdown and reorganization of the extracellular matrix (ECM), endothelial cells (ECs) sprouting, migration and adhesion junctions remodelling.[5] It has been shown that signals emitted by cardiomyocytes (CM) impact upon ECs function and modulate angiogenesis. Therefore, a fine-tuned regulation of communication between the different cell types in the heart is vital to ensure a proper vascularization of the heart required to sustain myocardial contraction.[6,7] Typically, the intercellular communication can occur directly, between adjacent cells, via gap junctions,[8] or indirectly, at long distances, through soluble factors and extracellular vesicles (EVs), including exosomes. These vesicles mediate intercellular communication under normal and pathological conditions by shuttling a wide range of functional lipids, proteins, mRNAs, and microRNAs (miRs).[9] It has been reported that exosomes play an important role in modulating angiogenesis, in different organs, including the heart.[10,11] For this reason, exosomes have emerged as potential therapeutic agents that can modulate ECs behaviour and elicit an angiogenic response. Indeed, progenitor and stem cell-derived exosomes present proangiogenic activity in cardiac ECs, namely in the context of hypoxia and ischaemia, where exosomes can mitigate injury.[12–15] However, the effect of exosomes secreted by CM subjected to ischaemia on ECs has never been described. In the present study we demonstrate *in vitro* and *in vivo* that exosomes produced by CM in ischaemia stimulate cardiac angiogenesis.

2. Methods

Detailed description of reagents and experimental procedures, cell lines, exosome purification, transmission electron microscopy (TEM), and fluorescence microscopy, nanotracking analysis (NTA), Western blot (WB), miR analysis, *in vitro* and *ex vivo* experiments, and animal studies are listed in Supplementary Material.

2.1 Exosomes and cell culture

Exosomes were isolated by differential centrifugation. Exosomes size and concentration was measured using NTA. Mouse Cardiac Endothelial Cell (MCEC) and Human Umbilical Vein Endothelial Cells (HUVEC) were incubated with exosomes isolated from H9c2 cells transfected with CD63-GFP, and uptake was determined by confocal microscopy. Primary cultures of cardiomyocytes were obtained from Wistar rat fetus (17–18 days of gestation) following the protocol described in Supplementary Material.

2.2 Functional assays

Cell monolayer integrity was assessed by transendothelial electrical resistance (TEER) and permeability assays. Zymography was used to detect MMP activity. The concentration of MMP-9 in isolated exosomes and EC supernatant was determined by ELISA assay. Proliferation was assessed by 5-bromo-2'-deoxyuridine (BrdU) incorporation and Ki67 immunostaining. Cell viability was determined by LIVE/DEAD® Viability/Cytotoxicity Kit. Cell migration was determined by the scratch assay. Angiogenic potential was assessed by ECs capillary-like formation on Matrigel. Angiogenic sprouting was evaluated by fibrin gel bead assay. *Ex vivo* microvessel sprouting from rat thoracic aortas in Matrigel. Chicken embryo chorioallantoic membrane (CAM) model was used to evaluate angiogenesis. *In vivo* vascular permeability was measured in CAM model by quantification of leakage of Evan's Blue Dye (EBD, Sigma). *In vivo* angiogenesis was assessed by implantation of matrigel in rat model and further quantification of hemoglobin content.

2.3 MI induction and exosome delivery

MI was induced by ligation of the left anterior descending coronary artery and exosomes were delivered into ischaemic region by intramyocardial injections. Blood vessel density was assessed by immunofluorescence detection of CD31, as previously detailed,[16] and *Griffonia Simplicifolia* Lectin I (GSL-I, Vector Laboratories) as described in Supplementary Material. Transthoracic echocardiography was performed 4 weeks after the surgery using a Vevo 2100 microultrasound platform coupled with a MS400 transducer (both FUJIFILM Visulasonics, Inc.). Four weeks after MI, diastole arrested heart were processed and sectioned according to previously published protocols.[16] In brief, infarct-size assessment was performed by staining paraffin sections according to the Trichrome Masson Stain kit (Sigma-Aldrich) with modifications described in Supplementary Material. Left Ventricle (LV) infarcted area and infarcted midline were measured using the semi-automatic MIQuant Software by a blinded operator and the final result presented as the average percentage throughout the LV.[16,17]

2.4 Statistical analysis

Data were displayed with mean ± SD on a bar or scatter dot plot (each dot represents one animal or independent experiment). Data was analysed with SPSS 22 (IBM) or GraphPad Prism 6 for Windows, version 6.01 (GraphPad Software, Inc.), graphs were assembled in GraphPad Prism 6. $P < 0.05$ was considered significant.

3. Results

3.1 Characterization of exosomes secreted by H9c2 and rat fetal cardiomyocytes

To evaluate whether ischaemia modulates the profile of vesicles released by CM we isolated, by differential ultracentrifugation, the exosomes secreted by myocardial H9c2 cells cultured either in control (Exo^{Ct}) or ischaemia-mimetic conditions (Exo^{Isch}) (hereinafter referred to as ischaemia), after which we used the NTA and TEM (*Figure 1A* and *B*, respectively) to assess the number, size and morphology of the vesicles. The presence of proteins typically enriched in exosomes and absence of calnexin in exosomal extract confirmed that the isolation procedure

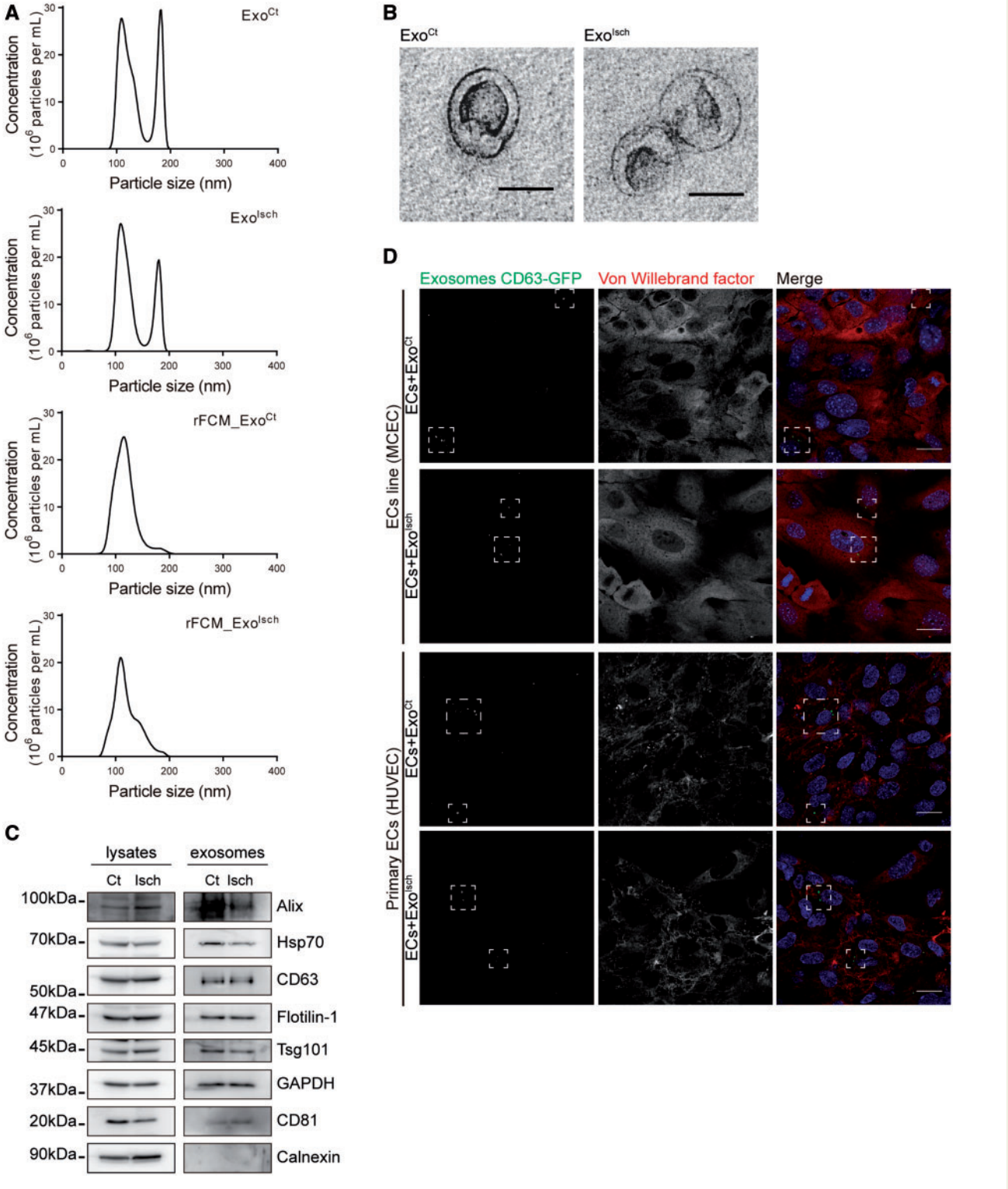

Figure 1 Ischaemia modulates the profile of exosomes secreted by H9c2 cells or cardiomyocytes in control or ischaemic conditions. Exosomes released by either myocardial H9c2 cells under control (Exo^{Ct}) or ischaemic (Exo^{Isch}) conditions or primary cultures of rat fetal cardiomyocytes (rFCM) cultured either under control ($rFCM\_Exo^{Ct}$) or ischaemia conditions ($rFCM\_Exo^{Isch}$) were isolated by differential ultracentrifugation and analysed by NTA, TEM, and WB. (*A*) Representative graph of exosome concentration (E^6 particles/mL) and size distribution of Exo^{Ct},Exo^{Isch}, $rFCM\_Exo^{Ct}$, and $rFCM\_Exo^{Isch}$ as measured by NTA. (*B*) Representative images of exosomes released by H9c2 cells visualized by TEM. Scale bars:100 nm. (*C*) Representative images of WB to assess the presence of enriched in exosomes and Calnexin in Exo^{Ct} and Exo^{Isch} and H9c2 lysates. (*D*) Representative confocal images of Exo^{Ct} and Exo^{Isch}, containing CD63-GFP, taken up by MCEC or HUVEC, highlighted with a white dashed-box. Scale bar:20 μm. (*A–D*) $n = 5$.

gave rise to a population of vesicles highly enriched in exosomes (*Figure 1C*). To evaluate if our isolation protocol excludes large protein aggregates or proteins nonspecifically associated with vesicles, we performed an extra purification step using a sucrose.[18] The presence of the exosomal marker CD63 mainly in the sucrose gradient (see Supplementary material online, *Figure* (SF) *1A*), and similar NTA profiles of vesicles obtained with either purification method (SF1B), confirm that the ultracentrifugation procedure is appropriate to isolate exosomes. Moreover, the absence of any effect of proteinase K on the vesicle profile revealed by NTA (SF1C), demonstrates that this exosomal fraction is devoid of protein aggregates. The presence of green puncta in the cytoplasm of MCECs or HUVEC revealed that exosomes secreted by H9c2 cells overexpressing CD63-GFP are internalized by ECs (*Figure 1D*). NTA shows that overexpression of CD63-GFP does not alter the profile of exosomes secreted by H9c2 cells (SF1D).

To validate the results obtained in H9c2 cells, we characterized the exosomes released by primary cultures of rat fetal cardiomyocytes (rFCM) cultured either under control (rFCM_Exo^{Ct}) or ischaemia conditions (rFCM_Exo^{Isch}), by NTA. These results show that the profile of exosomes secreted by H9c2 or rFCM is very similar, with both cells secreting less (9,32 ± 0,35 x 10^8particles/mL in Exo^{Ct} vs. 8,02 ± 0,3 x 10^8particles/mL in Exo^{Isch}; 8,29 ± 0,4 x 10^8particles/mL in rFCM_Exo^{Ct} vs. 7,02 ± 0,5 x 10^8particles/mL in rFCM_Exo^{Isch}) but slightly larger exosomes (126 nm in Exo^{Ct} to 137 nm in Exo^{Isch}; 111 nm in rFCM_Exo^{Ct}to 127 nm in rFCM_Exo^{Isch}) than control cells (*Figure 1A*).

3.2 Stimulation with Exo^{Isch} induces a transient decrease in TEER and promotes endothelial permeability

To assess the effect of H9c2-derived exosomes on MCEC barrier properties, we evaluated TEER and permeability to dextran in MCEC monolayers. Incubation with Exo^{Isch} lead to a significant TEER reduction between 1 and 12 h post-stimulation that returned to basal levels after 24 h (*Figure 2A*), whereas Exo^{Ct} did not affect TEER. The permeability assays demonstrate that after 1 h of incubation the permeability of MCEC to 10 and 70 kDa dextran is higher with Exo^{Isch} than Exo^{Ct}, after which the values tend to equalize with time. Following long periods of incubation (24 h), there was an inversion of permeability induced by exosomes, particularly evident in assays with 70 kDa dextran, with permeability induced by Exo^{Isch} being significantly lower than Exo^{Ct} (*Figure 2B* and *C*). Moreover, cells exposed to Exo^{Ct} for 2 h, present smooth lines of continuous staining for VE-cadherin and ZO-1 along cell-cell contacts (*Figure 2D*), suggesting strong adhesion, whereas ECs incubated with Exo^{Isch} had discontinuous and irregular VE-cadherin and ZO-1 distribution at the intercellular junctions. However, after 24 h of incubation, when compared with the results at 2 h, ECs exposed to Exo^{Ct} present a more irregular distribution and decrease staining for VE-cadherin and ZO-1, suggesting a disruption of barrier properties, whereas ECs treated with Exo^{Isch} show less discontinuous borders on the monolayer, accompanied by an increased labelling for VE-cadherin and ZO-1. Western blot analysis revealed that ECs stimulated with Exo^{Isch} have higher levels of ZO-1, VE-cadherin, and Occludin (SF2).

Strikingly, the effects described above with cell lines were confirmed in monolayers of primary ECs (HUVEC) stimulated with exosomes released by rFCM. Similarly to MCEC, rFCM_Exo^{Ct} did not affected HUVEC TEER, whereas, rFCM_Exo^{Isch} promoted a significant TEER reduction from 1 to 12 h post-stimulation in primary ECs, values that reverted to basal level after 24 h (*Figure 2E*). Moreover, permeability assay results showed that after 1 h of incubation the permeability to 10 and 70 kDa dextran is higher in cells stimulated with rFCM_Exo^{Isch} than rFCM_Exo^{Ct} (*Figure 2G* and *H*). Also the VE-cadherin staining was higher in HUVEC incubated with rFCM_Exo^{Isch} than rFCM_Exo^{Ct}, supporting the idea that for long periods of incubation ischaemic exosomes strengthen cell-cell adhesions (*Figure 2F*). Altogether these data demonstrate that Exo^{Isch} cause a transient disruption of the endothelial barrier, with increased paracellular permeability and decreased TEER, after which the barrier properties are re-established or even strengthened.

3.3 Exo^{Isch} promote ECM degradation

Previous studies reported that exosomes may carry and deliver active MMPs, namely MMP-2 and -9 that favour angiogenesis.[13,19] The results presented in *Figure 3A* and *B* (gelatine zymography) show that Exo^{Isch} contain higher levels of MMP-9 and MMP-2, in comparison with Exo^{Ct}. In agreement, ELISA data demonstrate that Exo^{Isch} present 2 times more MMP-9 than Exo^{Ct} (*Figure 3C*), suggesting that exosomes released by CM subjected to ischaemia promote the degradation of ECM. Furthermore, we show that Exo^{Isch} enhance the secretion of MMP-2 and MMP-9 by MCEC (*Figure 3D–E*, and *F*). These findings ascribe to exosomes a role in ECM degradation during ischaemia, namely by carrying MMPs released by CM and/or by inducing MMPs secretion by ECs.

3.4 Exo^{Isch} promote ECs proliferation and survival upon stress

We subsequently tested whether exosomes released by CM regulate ECs proliferation using two different techniques, Ki67 staining, which is present in all active phases of the cell cycle, and BrdU incorporation. Both approaches demonstrated that Exo^{Isch} significantly increased the proliferation of MCEC, compared with Exo^{Ct} (*Figure 3G* and *H*). Furthermore, we evaluated the impact of Exo^{Ct} and Exo^{Isch} on the capacity of cells to respond to oxidative stress, often implicated in heart disorders, including myocardial ischaemic syndromes and reperfusion-associated lesions.[20] As shown in *Figure 3I*, Exo^{Isch} significantly improve ECs viability when subjected to oxidative stress, compared to cells pretreated with Exo^{Ct}, suggesting that Exo^{Isch} can be cardioprotective.

3.5 Exo^{Isch} promote ECs migration, capillary-like tube, and sprouting formation

To assess the impact of CM-released exosomes on ECs behaviour and angiogenic potential capacity, we evaluated ECs migration, tube formation and sprouting. The results presented in *Figure 4A* and *B*, demonstrate that MCEC stimulated with Exo^{Isch} migrate faster than those incubated with Exo^{Ct}. Moreover, Exo^{Isch} exhibited an increased capacity to induce the formation capillary-like structures, on a classical Matrigel assay, as demonstrated by the presence of higher number of meshes and branch points, as well as longer tube-like segments (*Figure 4C* and *D*).

To evaluate the sprouting of ECs, an important step of the angiogenic process, we used the three-dimensional *in vitro* angiogenesis system and the *ex vivo* aortic ring assay. After 24 h of incubation of exosomes with ECs adhered to *beads*, Exo^{Isch} resulted in the formation of longer and higher number of sprouts, as compared to Exo^{Ct} (*Figure 4G* and *H*). Also in transverse sections of rat aortic tissue embedded in Matrigel, after 5 days of incubation, Exo^{Isch} significantly increased in the number of sprouts, when compared with Exo^{Ct} (*Figure 4J* and *K*). These results were confirmed in HUVEC, where rFCM_Exo^{Isch} induced a robust angiogenic response when compared with rFCM_Exo^{Ct}, assessed either by tubulation and sprouting assays (*Figure 4E–F* and *I*, respectively).

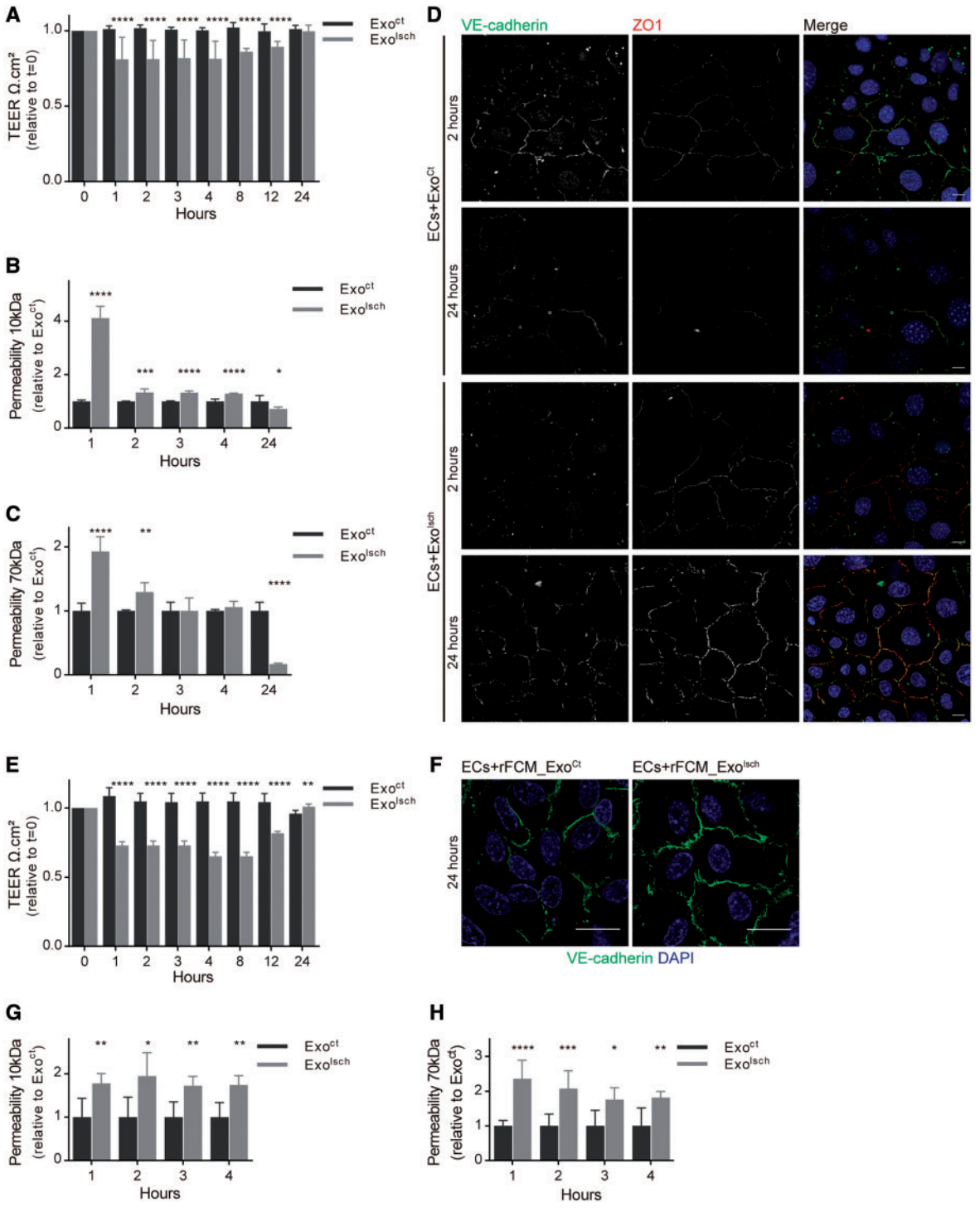

Figure 2 Ischaemia-derived exosomes decrease TEER and increase endothelial permeability. (*A–D*) MCEC tight monolayer was stimulated with Exo^{Ct} or Exo^{Isch} (time 0). (*A*) TEER was recorded over 24 h and normalized to the time 0 values ($n = 5$–19). (*B*, *C*) Macromolecular flux across cell monolayer was assessed using RITC-dextran(10 kDa). (*B*) and FITC-dextran(70 kDa) (*C*) at different time points after Exo^{Ct} and Exo^{Isch} exposure ($n = 5$). (*D*) Subcellular distribution of the adherens junctional protein VE-cadherin (green) and the tight junction protein ZO-1 (red), evaluated using immunofluorescent confocal microscopy, in cells exposed either to Exo^{Ct} or Exo^{Isch} for 2 or 24 h. Nuclei were stained with DAPI(blue). Scale bar:10 μm. (*E–H*) Primary HUVEC tight monolayer was stimulated with rFCMExo^{Ct} or rFCMExo^{Isch}(time0). (*E*) TEER was recorded over 24 h and normalized to the time 0 values ($n = 5$). (*F*) Subcellular distribution of the adherens junctional protein VE-cadherin (green) was evaluated using immunofluorescent confocal microscopy, in cells exposed either to rFCM_Exo^{Ct} or rFCM_Exo^{Isch} for 24 h. Nuclei were stained with DAPI (blue). Scale bar:20 μm. (*G*, *H*) Macromolecular flux across ECs monolayer was assessed using RITC-dextran(10 kDa) (*G*) and FITC-dextran(70 kDa) (*H*) at different time points after with rFCM_Exo^{Ct} or rNCM_Exo^{Isch} exposure ($n = 5$). Results represent mean ± SD. *$P < 0.05$, **$P < 0.01$, ***$P < 0.001$, and ****$P < 0.0001$ relative to Exo^{Ct} or rFCMExo^{Ct} at the same time-point in all graphs. *t*-test (Holm-Sidak's).

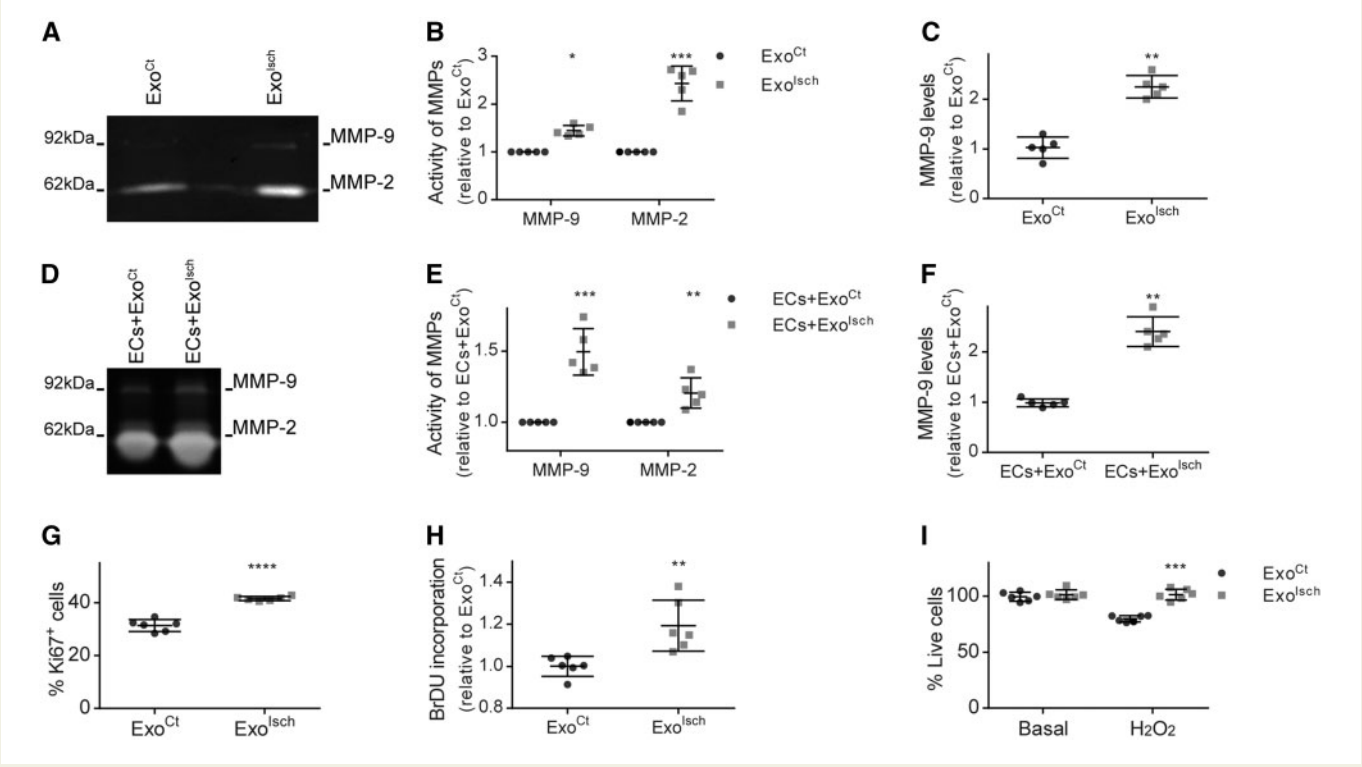

Figure 3 Ischaemic exosomes promote extracellular matrix degradation and ECs proliferation and survival upon stress. (*A*) Gelatin zymography was used to detect MMP-9 and MMP-2 in Exo^{Ct} and Exo^{Isch}. (*B*) Density of lytic bands corresponding to MMP-9 and -2 was quantified and plotted in a graph ($n = 5$). (*C*) MMP-9 levels were quantified by ELISA in Exo^{Ct} and Exo^{Isch} ($n = 5$). (*D–F*) Conditioned media from ECs pre-treated with Exo^{Ct} or Exo^{Isch} for 12 h was collected to evaluate MMP release by ECs. (*D*) Collected ECs conditioned media was used to perform gelatin zymography for MMP-9 and MMP-2. (*E*) Density of lytic bands corresponding to MMP-9 and -2 was quantified and plotted in a graph ($n = 5$). (*F*) MMP-9 released by ECs was quantified by ELISA ($n = 5$). (*G–I*) ECs were cultured with Exo^{Ct} or Exo^{Isch} for 8 h, after which proliferation and resistance to stress was assessed. (*G*) Cell proliferation was evaluated as the percentage of Ki67 positive cells ($Ki67^{+}$) relative to total number of cells (DAPI), ($n = 6$). (*H*) ECs proliferation was evaluated by BrDU incorporation. Absorbance values were normalized to Exo^{Ct} ($n = 6$). (*I*) ECs pre-treated with Exo^{Ct} or Exo^{Isch} were incubated with H_2O_2. Live cells were detected by fluorescence intensity of calcein AM and the results normalized to the Exo^{Ct} under basal conditions, ($n = 6$). Results represent mean ± SD. (*B*, *E*, and *I*) *t*-test (Holm-Sidak's); (*C*, *F*, *G*, and *H*) 2-tailed *t*-test. $^{*}P < 0.05$, $^{**}P < 0.01$, $^{***}P < 0.001$, and $^{****}P < 0.0001$ relative to Exo^{Ct}.

Together, we provide strong evidence that exosomes released by CM subjected to ischaemia promote cardinal features of angiogenesis including EC migration, sprouting and formation of capillary-like structures.

3.6 miRs present on exosomes modulate the angiogenic response

In an attempt to unveil the players involved in exosome-induced angiogenesis, we investigated the profile of miR sorted in Exo^{Ct} and Exo^{Isch}. From 752 miRs tested, we detected a total of 172 present in Exo^{Ct} and Exo^{Isch}, with only 7 miRs of them being differentially represented in Exo^{Ct} and Exo^{Isch} (*Figure 5A*). Pathway enrichment analysis associated up-regulated miRs with pathways related with cell proliferation and differentiation (see Supplementary material online, *Table* (ST) *1*). GO-term enrichment analysis associated these same targets with genes related to heart development, response to shear stress by fluids and signal transduction (ST2), and genes involved in signal transduction via transcription factors or membrane receptors (ST3). The down-regulated miRs are mainly associated with cancer and cell proliferation pathways (ST4), as well as nucleic acid binding processes (ST5-6). Furthermore, we validated the results of the screening approach in H9c2 and rFCM, concerning the two relatively most abundant miRs present on ischaemic exosomes, miR-143, and miR-222. We confirmed by qPCR that ischaemic exosomes released by H9c2 and rFCM are enriched in miR-143 and miR-222 (*Figure 5B* and *C*, respectively), when compared with exosomes secreted by cells maintained under basal conditions.

Importantly, the enrichment in miR-143 and miR-222 as well as the pro-angiogenic properties of Exo^{Isch} are maintained when the exosomal extract is treated with RNase and proteinase K, to degrade free miRNA and dissociate complexes which might otherwise shield RNA, prior to RNA isolation and quantification (SF3A-B and SF4). Moreover, to clarify if miRs were present in exosomes and exclude its presence in protein aggregates, we also quantified miR-143 and miR-222 levels after an extra purification step using the sucrose cushion method. The results demonstrate that the levels of miRNA in the pellet are residual and, more important, in the exosomal fraction recovered in the cushion, the relative enrichment of miR-143 and -222 in Exo^{Isch} compared to Exo^{Ct} was maintained (SF3C).

These results support the idea that exosome-mediated response is mediated, at least partially, by miRNA loaded in the vesicles.

Subsequently, we investigated whether these two miRs (miR-143 and miR-222) have an impact on the angiogenic process. The results

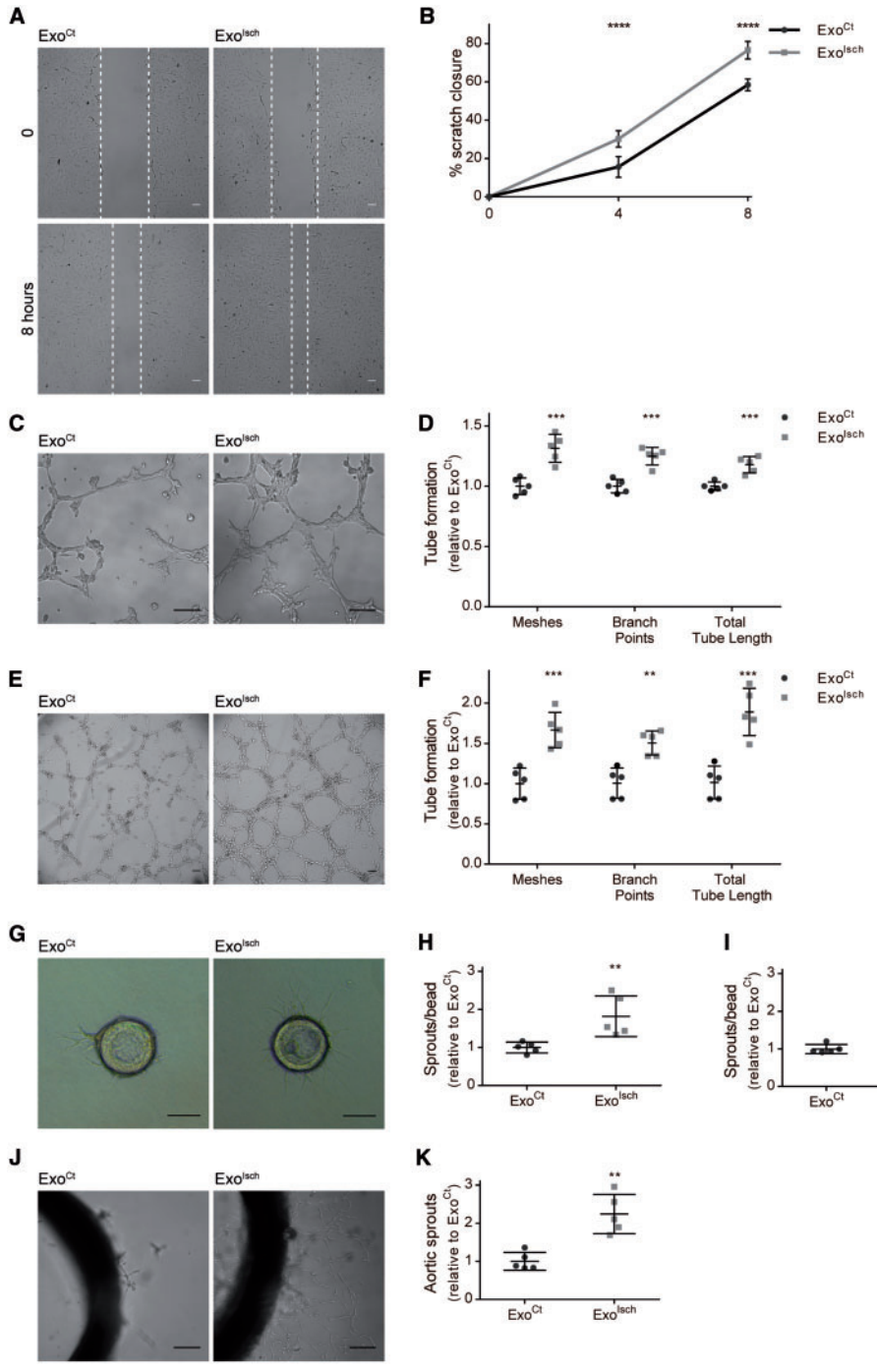

Figure 4 Ischaemic exosomes promote ECs migration and formation of capillary-like tubes and sprouting formation. (*A–B*) MCEC migration was monitored 8 h after the scratch in cells maintained in medium supplemented with Exo^{Ct} and Exo^{Isch}. (*A*) Representative phase-contrast images are shown. Scale bar: 100 μm. (*B*) Distance measurements were performed at the indicated times after the scratch, percentage of closure was calculated and plotted ($n = 8$). (*C–F*) Capillary-like tube formation assay on Matrigel was assessed 5–8 h after ECs seeding with exosome-depleted medium supplemented with exosomes. (*C*, *D*) MCECs were stimulated with Exo^{Ct} and Exo^{Isch}. (*C*) Representative phase-contrast images. Scale bar:100 μm. (*D*) Quantitative assessment of total number of meshes, branch points and tube-like segments length, results normalized to Exo^{Ct} ($n = 5$). (*E*, *F*) HUVECs were stimulated with rFCM_Exo^{Ct}or rFCM_Exo^{Isch}. (*E*) Representative phase-contrast images, Scale bar: 100 μm. (*F*) Quantitative assessment of total number of meshes, branch points and tube-like segments length, results normalized to rFCM_Exo^{Ct} ($n = 5$). (*G–I*) ECs adhered on beads in three-dimensional fibrin gels were incubated with exosomes for 24 h. (*G*) Representative phase-contrast images of MCECs stimulated with Exo^{Ct} and Exo^{Isch}. Scale bar: 100 μm. (*H*) Quantitative assessment of number of MCECs sprouts per bead ($n = 5$). (*I*) Quantification of sprouts per bead of HUVECs stimulated with rFCM_Exo^{Ct} or rFCM_Exo^{Isch} ($n = 5$). (*J*, *K*) Cultures of rat aortic rings were stimulated with Exo^{Ct} and Exo^{Isch} for 5 days, after which aortic rings were fixed and number of sprouts counted. (*F*) Representative phase-contrast images. Scale bar: 100 μm. (*G*) Quantitative assessment of number of sprouts per aortic ring ($n = 5$). Results represent mean ± SD. (*B*, *H*, *I*, and *K*) 2-tailed *t*-test; (*D* and *F*) *t*-test (Holm-Sidak's) $^{**}P < 0.01$, $^{***}P < 0.001$, and $^{****}P < 0.0001$.

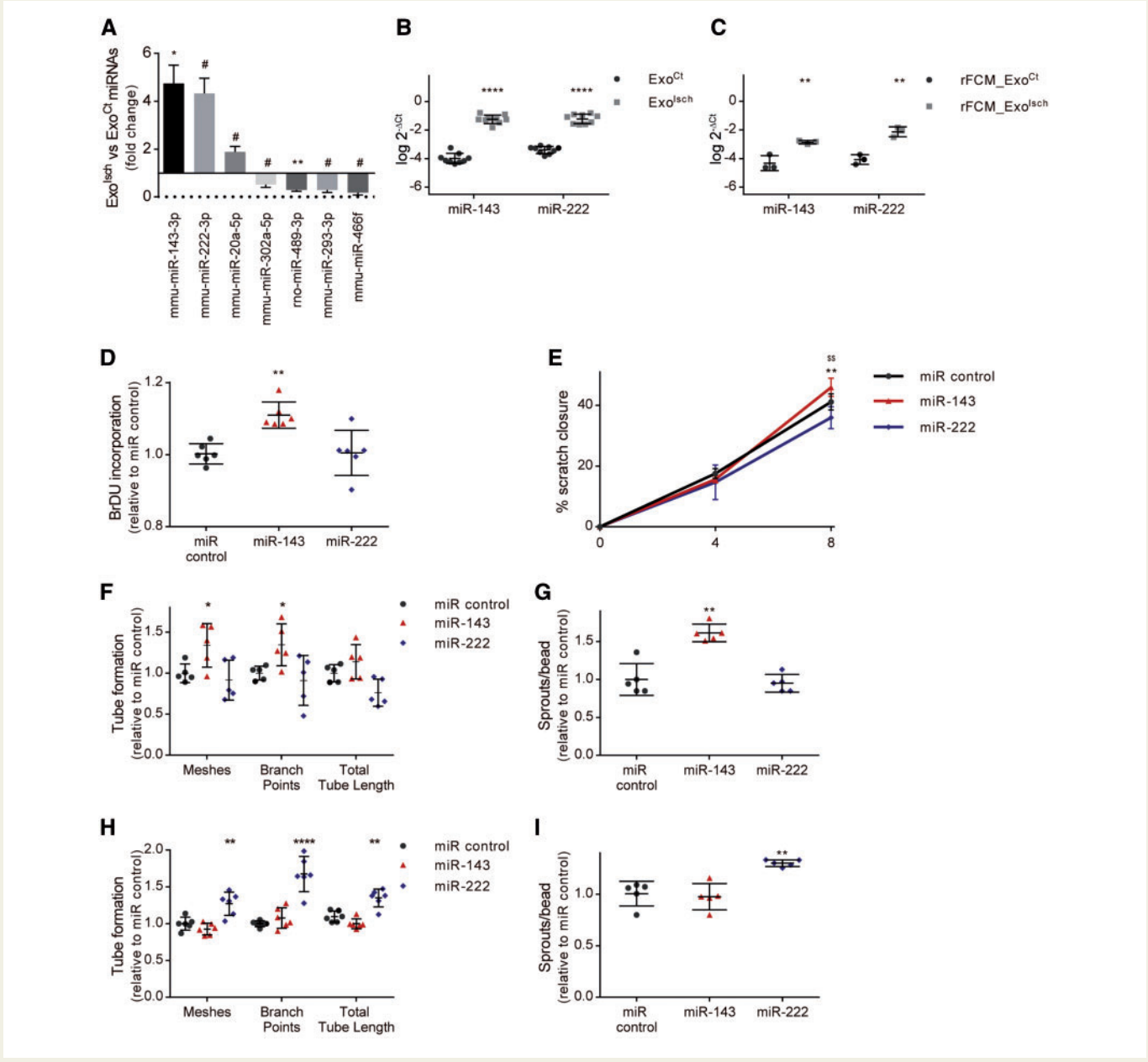

Figure 5 miRs exosomal content modulate the angiogenic response. (*A*) Relative expression of miRs presented in Exo^{Ct} and Exo^{Isch} of H9c2, ($n = 3$) *P*-values were calculated by using Benjamin-Hochberg False Discovery Rate (FDR). (*B*, *C*) miR-143 and miR-222 levels, were determined by quantitative polymerase chain reaction (qPCR) in and expressed as logarithmic values of $2^{-\Delta Ct}$ using U6 as a normalizer, in (*B*) Exo^{Ct} and Exo^{Isch} of H9c2 and (*C*) rFCM_Exo^{Ct} and rFCM_Exo^{Isch}. (*D–F*) MCECs were transfected with miR-143 or miR-222 and cultured for 24 h after which proliferation, migration, tubulation, and sprouting was assessed. (*D*) ECs proliferation was evaluated by BrDU incorporation ($n = 6$). (*E*) ECs migration by scratch assay, distance measurements were performed at the indicated times after the scratch, percentage of closure was calculated and plotted in a graph ($n = 6$) $$miR-222 to miR Control. (*F*) Capillary-like tube formation assay on Matrigel was assessed 5–8 h after ECs seeding. Quantification of total number of meshes, branch points and tube-like segments length ($n = 5$). (*G*) Assessment of MCECs sprouts adhered on beads in three-dimensional fibrin gels ($n = 5$). (*H–I*) HUVECs were transfected with miR-143 or miR-222 and cultured for 24 h after which tubulation and sprouting was assessed. (*H*) Capillary-like tube formation assay on Matrigel was assessed. Quantification of total number of meshes, branch points and tube-like segments length was performed ($n = 6$). (*I*) Number of HUVECs sprouts upon upregulation of miR-143 and miR-222 was performed in at least 5 beads per condition in each experiment ($n = 5$). (*A–C*) Results were normalized with the spike-in RNA control. (*D–I*) Results were normalized to miR Negative Control (miR Control). Results represent mean ± SD. (*B–I*) *t*-tests (Holm-Sidak's). $^{\#}P < 0.1$, $^{*}P < 0.05$, $^{**}P < 0.01$, and $^{****}P < 0.0001$.

obtained in MCEC demonstrated that stimulation with miR-143 significantly increased cell proliferation (*Figure 5D*) and migration (*Figure 5E*), and promoted the formation of capillary-like structures (*Figure 5F*), and cell sprouting (*Figure 5G*). None of these parameters were significantly altered in MCEC stimulated with miR-222. The increase in intracellular levels of miRNAs -143 and -222 after transfection demonstrated those miRs were taken up by ECs (SF5). Concerning HUVEC, we observed that miR-222 promoted tubulation and sprouting, whereas

miR-143 had no significant impact in any of these parameters (*Figure 5H–I*). Despite apparently contradictory, these results indicate that these miRs can be, at least partially, responsible for the pro-angiogenic effect of Exo^{Isch}.

3.7 Exo^{Isch} promote angiogenesis *in vivo*

Next, we evaluated the angiogenic potential of Exo^{Isch} *in vivo*, using two distinct angiogenic assays, the CAM and the Matrigel plug assays. For the CAM assay, fertilized chick eggs were inoculated with Exo^{Ct} or Exo^{Isch} and the angiogenic response evaluated after 72 h. Exo^{Isch} promote a 30% increase in CAM vascular density when compared to Exo^{Ct} treatment (*Figure 6A* and *B*). Furthermore, intravenous injection of chick embryos with EBD demonstrated that new vessels formed upon stimulation with Exo^{Isch} present proper endothelial barrier similarly to the response to Exo^{Ct} (*Figure 6C*).

Furthermore, the angiogenic role of Exo^{Isch} *in vivo* was confirmed by the evaluation of blood vessel growth in Matrigel plugs implanted in rats. Matrigel containing Exo^{Ct} or Exo^{Isch} was injected s.c., and after 1 week were excised and photographed to assess the presence of blood vessels. The Matrigel plugs containing Exo^{Isch} exhibited bright red colour indicating blood-perfused vessels whereas Exo^{Ct}-containing plugs presented light yellowish colour that is correlated with the limited formation of new blood vessel (*Figure 6D*). Additionally, a quantitative analysis of the haemoglobin content inside the Matrigel plugs demonstrated that Exo^{Isch} promote a two-fold increase in the haemoglobin content in Matrigel (*Figure 6E*), reinforcing the idea that Exo^{Isch} present a pro-angiogenic potential *in vivo*.

3.8 Exo^{Isch} promote angiogenesis following MI

To assess the beneficial potential of exosomes produced by ischaemic CM, Exo^{Ct} or Exo^{Isch} were delivered to the myocardium of mice subjected to MI at the onset of injury. Survival rate of animals treated with Exo^{Isch} was higher, which may relate with a protective effect from ischaemia (SF6). One month following MI, mice subjected to Exo^{isch} treatment showed a tendency for an increase in ejection fraction, however due to changes in preload, this does not result in an improvement of systolic cardiac function as assessed by cardiac output (CO) (*Figure 7A* and *B*), likely owing to the fact that left ventricular chamber of Exo^{Ct} animals was more dilated (*Figure 7C* and *D* and ST7). Most importantly angiogenesis was enhanced following Exo^{Isch} treatment as shown by higher numbers of CD31^{+} cells in the infarcted region (*Figure 7E–F*) and of lectin-perfused vessels in the infarction border zone (*Figure 7G–H*) of Exo^{Isch}-treated mice. As proangiogenic factors may also promote a reduction on cardiac fibrosis and remodelling after MI, the percentage of collagen deposition was quantified in representative sections of the LV (*Figure 7I*). No differences were detected across groups (*Figure 7J–K*). Altogether, these results are entirely consistent with our hypothesis that exosomes produced by ischaemic CM promote angiogenesis following acute MI thus supporting blood perfusion to the myocardium.

4. Discussion

A tightly regulated and balanced crosstalk between the different cells that form the heart is vital for cardiac function. It is well established that a

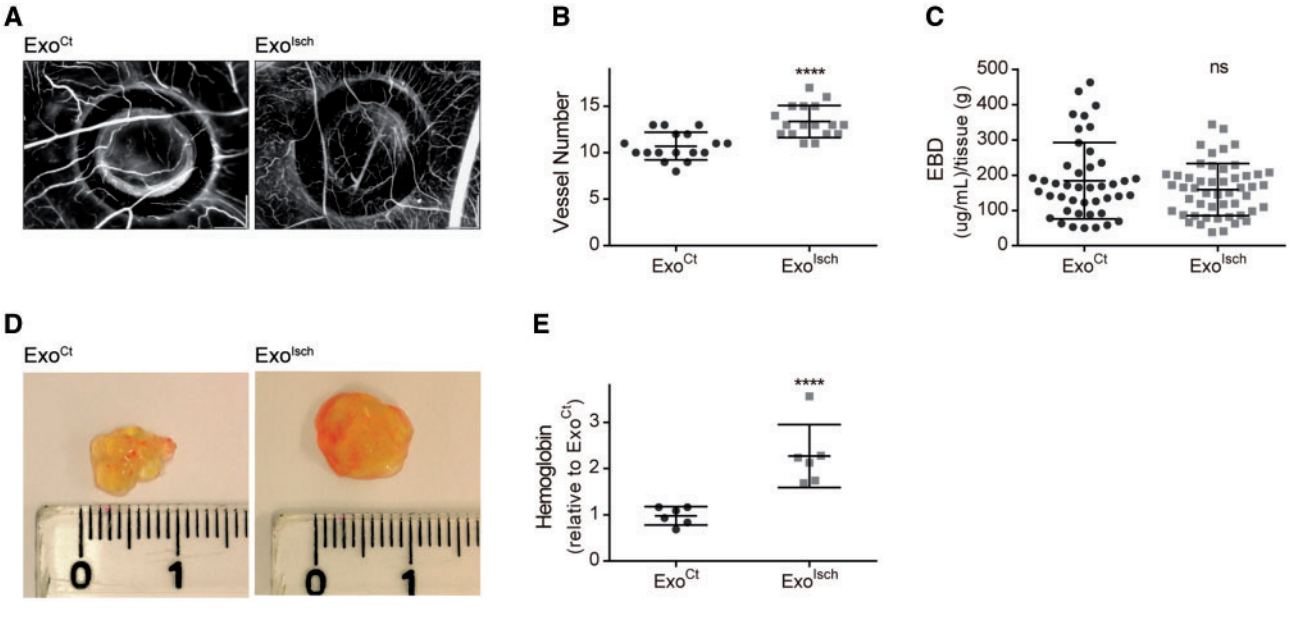

Figure 6 Exo^{Isch} promote angiogenesis *in vivo*. (*A–C*) Fertilized chicken eggs were inoculated with Exo^{Ct} or Exo^{Isch} for 72 h. (*A*) Representative images of the vascular branches in chicken embryo chorioallantoic membrane (CAM). 20x magnification. (*B*) Quantification of the newly formed blood vessels was performed by counting of visible branches. (*C*) After incubation period chick embryos were injected intravenously with Evan's Blue Dye (EBD) followed by perfusion with saline. The amount of EBD in the underlying the rings was quantified and used as a measure of vessel leakage ($n = 5$ to 8 eggs per experiment). (*D*, *E*) Matrigel enriched with Exo^{Ct} or Exo^{Isch} was implanted in rat flank and excised after 7 days. (*D*) Representative images of excised matrigel plugs containing either Exo^{Ct} or Exo^{Isch}. (*E*) Angiogenesis was quantified by measuring the haemoglobin content in the matrigel plugs. ($n = 6$). Results represent mean ± SD. (*B*, *C*, *E*) 2-tailed *t*-test; ****$P < 0.0001$.

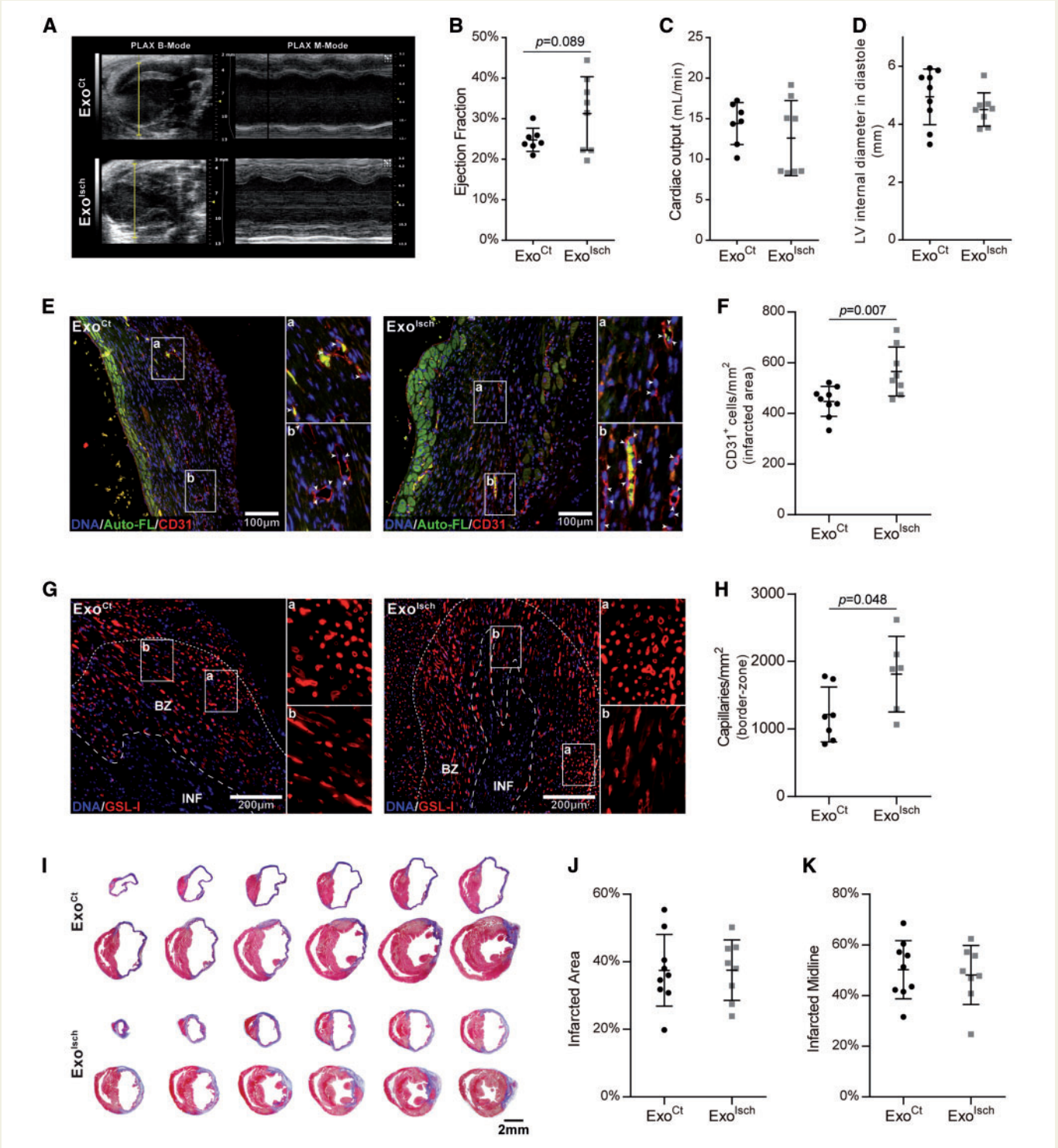

Figure 7 Exo^{Isch} stimulates angiogenesis and improves LV function 4 weeks after MI. (*A*) Representative B-mode and M-mode images of parasternal long-axis (PLAX) view (30 Mhz). (*B*) Ejection fraction determined using the Simpson's method in PLAX view. (*C*) Cardiac output determined using the Simpson's method in PLAX view. (*D*) LV internal diameter at end diastole determined in Parasternal short-axis view, M-mode. (*E*) Representative sections of CD31 immunolabelling in the infarcted free wall. (*F*) Quantification of CD31 nucleated cells (arrowheads) in thein the infarcted area (INF) (3 sections per animal, average 1.2 mm^2 of infarcted tissue analysed per heart). (*G*) Representative images of GSL-I perfused capillaries in the INF and borderzone (BZ). (*H*) Quantification of GSL-I perfused vessels in the BZ (3–4 sections per animal, average 0.6 mm^2 analysed per heart). (*I*) Representative transverse heart sections stained with Masson's Trichrome. Collagen deposition (scarring) is identified in blue. (*J*) Infarcted area and (*K*) infarcted midline quantification across LV of arrested hearts using MIQuant. N presented for each experiment; final number of animals of Exo^{Ct}=9 and Exo^{Isch}=8; PLAX view was not successfully acquired in 2 animals of the Exo^{Ct} group ($n = 7$); lectin perfusion was attained in a subset of animals (Exo^{Ct}=7 and Exo^{Isch}=6). Results represent mean ± SD; each dot represents one animal. Experimental groups passed the Shapiro-Wilk normality test ($P > 0.05$). *P* value is shown for 2-tailed *t*-test; whenever equality of variances cannot be assumed (Levene's test $P < 0.05$, EF), adjusted *P* value is shown instead.

panoply of paracrine signals secreted by cardiomyocytes, namely growth factors, hormones and genetic material, can modulate vasculature dynamic. For example, physiological cardiac hypertrophy relies on a fine-tuned interplay between CM and ECs, which promotes the formation of new vessels required to supply the needs of enlarged CM. However, in the context of pathological hypertrophy, the growth of CM mass is not accompanied by a proper angiogenesis process, thus contributing to cardiac dysfunction due to a deficit in blood supply. For this reason, defects in capillary density have been associated with the transition from a compensated to a decompensated cardiac hypertrophy.[4] Although the role of soluble factors-mediated communication between CM and ECs in heart physiopathology is relatively well studied, the involvement of exosomes in this interplay remains largely elusive. In this study we show that exosomes secreted by CM subjected to ischaemia promote angiogenesis, both *in vitro* and *in vivo*. Furthermore, we provide strong evidence that miR-222 and miR-143, the relatively most abundant miRs in ischaemic exosomes, account for the angiogenic process.

The involvement of extracellular vesicles in angiogenesis is not without precedents. It was previously shown that exosomes derived from bone marrow-derived mesenchymal stem cells (BMSCs) and induced pluripotent stem cell-derived mesenchymal stem cells (iMSCs) can promote angiogenesis in ischaemia conditions and attenuate tissue injury after an ischaemic insult.[15,21] Moreover, exosomes released by H9c2 cells in glucose-deprivation induce the transcription of pro-angiogenic genes in ECs.[22]

In the present study, we evaluated the effect of ischaemia on exosomes released by two different cell types: a cardiac myoblast cell line (H9c2) and primary cultures of CM. In both cases, we demonstrated that ischaemia affects the size and number of secreted vesicles, as well as their protein and miR content. Importantly, we showed that the exosomes secreted by both cell types are enriched in miR-222 and miR-143.

It is conceivable that ischaemia-induced changes in the miR profile of exosomes reflects a highly selective sorting of miR into exosomes as part of an orchestrated approach to specifically modulate the activity of distant target cells, in order to preserve organ homeostasis. According to our model, as part of a coordinated strategy, CM under ischaemia release miR that sustain the formation and growth of new vessels to replenish blood supply to the deprived area. In accordance, it was previously demonstrated in pulmonary artery ECs that exosome-derived miR-143, or direct transfection of premiR-143, induced cell migration and capillary-like tube formation, and protects against cell death, thus ascribing to this miR pro-angiogenic properties.[23] Concerning miR-222 the results are somehow contradictory. The anti-angiogenic effect of the cluster miR221/miR-222 was demonstrated in diabetes-inducing inhibition of vessel formation and in miR-221/miR-222-transfected HUVEC, where this miR promoted lower migration potential, proliferation and tubule formation capacity.[24,25] In contrast, studies carried out by Yang *et al.* showed that conditioned medium from miR-221/miR-222-overexpressing cells induced an increase in the formation of tube-like structures by HUVECs.[26] Additionally, conditioned medium from cells with downregulation of miR-222 (by overexpression of anti-miR-222) was shown to decrease tube-like formation in HUVECs.[27] These apparent conflicting data may derive from the approaches used to evaluate the role of miRs in angiogenesis, i.e. direct transfection vs. conditioned medium. It is likely that the single miR transfection does not entirely mimic the effect of miR-enriched conditioned medium and/or exosomes. Our results show that the angiogenic potential of ischaemic exosomes, enriched in miR-222, and miR-143, is very similar in both MCEC and HUVEC. However, when the impact of each of the two miRs was evaluated individually, the results were slightly different and isolated miRs did not entirely recapitulate the effect of exosomes. While the miR-222 presents a pro-angiogenic potential in HUVEC (with no significant effect on MCEC), the miR-143 promotes angiogenesis only in MCEC. This is not surprisingly, since the approach using single miR does not take into consideration other biomolecules present in exosomes, namely other miRs, lipids and proteins, the profile of whose can change with ischaemia and can differentially affect angiogenesis. Indeed, when stimulated with exosomes the cells are exposed to a myriad of factors acting simultaneously, leading to a global comprehensive effect. However, when using a single miR a more complex and orchestrated response involving a multitude of effects elicited by the combination of various molecules present at exosomes is lost. The apparent different effect of miR-222 and miR-143 in two distinct ECs can be due to the diverse roles these miRs play either in large vessels or microvasculature, HUVEC and MCEC, respectively.

In addition to the miR content, it is likely that the effect of exosomes on ECs depends on the protein content. For example, changes in the profile of proteins on the surface of exosomes can modulate the interaction of the vesicles with the acceptor cells, thus dictating the final effect. It is plausible that the mode of exosome docking at cell surface might not only mediate the selective access of exosomes into the cytoplasm of ECs but also trigger signalling cascades that would culminate in angiogenesis. Besides activation of signalling pathways, it is plausible that a decrease in the levels of short-lived proteins, with important role in angiogenesis, after a few hours of treatment with exosomes or miRNAs, account for the rapid effect of exosomes. It is worth noting that Connexin43 (Cx43), that is known to undergo a profound remodelling upon heart ischaemia and reperfusion, can facilitate the release of exosomal content into target cells.[28] Hence, it is conceivable that ischaemia-mediated changes in the content of Cx43 in exosomes determine the interaction and the effect on target cells.

It was previously shown that cardiomyocyte progenitor cells (CMPCs)-derived exosomes contain several MMPs, suggesting that exosomes themselves are able to breakdown the ECM or to activate pro-active MMPs.[13] In accordance, we observed that Exo^{Isch} not only carry MMPs, namely MMP-2 and -9, capable of degrading matrix but also have the capacity to promote the production and release of MMPs by ECs. Additionally, we show that Exo^{Isch} start by inducing a transient disruption of endothelial barrier properties followed by the strengthening of inter-endothelial junctions. Consistent with the cell-based approaches, *in vivo* studies, using the CAM and Matrigel plug models, demonstrate that Exo^{Isch} promote an increase in the formation of new functional non-leaky vessels. Previous studies have demonstrated that exosomes derived from stem and progenitor cells injected intramyocardially reduce myocardial ischaemia/reperfusion injury through proangiogenic effects.[29,30] However, the effect of ischaemic exosomes on heart angiogenesis has never been addressed. Our data show that the intramyocardial delivery of ischaemic exosomes increases the frequency of perfused vessels in the infarct border zone as well as the number of $CD31^+$ cells in the ischaemic region when compared to the control exosomes-treated group. Of note, although in physiological conditions, myocardial $CD31^+$ cells are ECs, in an injury scenario it is conceivable that this compartment may also include bone marrow-derived $CD45^+CD31^+$ cells, which have been previously associated with proangiogenic properties.[31,32] Indeed, although the effect of Exo^{Isch} on ECs was undoubtedly demonstrated *in vitro*, it is likely that in an injury scenario other mechanisms may also mediate the observed pro-angiogenic effects, namely through the modulation of inflammatory response. Notwithstanding, no

significant changes in either infarct size and cardiac function were observed, possibly because the amount of revascularization elicited by the delivered exosome dosage might not have been enough to halt cardiac remodelling alone. Nevertheless, these results strongly support our main conclusion that exosomes secreted by CM subjected to ischaemia promote cardiac angiogenesis following MI. Despite the biological impact of our results, the fact that the amount of exosomes used likely exceeds that found in 'pathophysiological' conditions *in vivo* might constitute a drawback in terms of clinical significance. Moreover, in our study we used the LAD permanent occlusion MI model, rather than an ischaemia/reperfusion model that could be more clinical relevant, since our main purpose was just to create more favourable experimental conditions to assess the formation of new vessels in the heart (the high vessel density of non-infarcted myocardium would most likely mask the evaluation of the pro-angiogenic potential of exosomes).

To the best of our knowledge, this is the first study showing that exosomes released by ischaemic CM promote angiogenesis, which can constitute a significant contribution to elucidate the mechanisms underlying the growth of new vessels in the heart. Although the determinants of development of CCC remain controversial, it has been associated with fluid shear stress on ECs and the attraction of monocytes. However, it is conceivable that CM subjected to a chronic and prolonged stress insult produce exosomes that sustain the growth of new vessels underlying CCC. It can be also speculated that the growth of new vessels implicated in healthy hypertrophy is modulated by exosomes released by hypertrophic cardiomyocytes, namely the miR-222 and miR-143, known to promote physiological cardiac hypertrophy.[33] Overall, our study can open new avenues towards the use of exosomes as cell-free therapeutic agent for the induction of local neovascularization after MI.

Supplementary material

Supplementary material is available at *Cardiovascular Research* online.

Acknowledgements

The authors are indebted to Cláudia Machado (i3S/INEB) for the help with heart tissue sectioning. In vivo echocardiography data was acquired using equipment made available and maintained by the Bioimaging Center for Biomaterials and Regenerative Therapies (b.IMAGE).

Conflict of interest: none declared.

Funding

This work was supported by European Regional Development Fund (FEDER) through the Operational Program for Competitiveness Factors (COMPETE) [HealthyAging2020 CENTRO-01-0145-FEDER-000012-N2323, POCI-01-0145-FEDER-016385, POCI-01-0145-FEDER-007440 to CNC.IBILI, POCI-01-0145-FEDER-007274 to i3S/INEB and NORTE-01-0145- FEDER-000012 to T.L.L.]; national funds through the Portuguese Foundation for Science and Technology (FCT) [PTDC/SAU-ORG/119296/2010, PTDC/NEU-OSD/0312/2012, PESTC/ SAU/UI3282/2013-2014, MITP-TB/ECE/0013/2013, FCT-UID/NEU/04539/2013], PD/BD/52294/2013 to T.M.R.R., SFRH/BD/85556/2012 (co-financed by QREN) to V.C.S]; Lisboa Portugal Regional Operational Programme (LISBOA 2020) and Norte Portugal Regional Operational Programme (NORTE 2020), under the PORTUGAL 2020 Partnership Agreement; and by INFARMED Autoridade Nacional do Medicamento e Produtos de Saúde, I.P. [FIS-FIS-2015-01_CCV_20150630-157].

References

1. Mozaffarian D, Benjamin EJ, Go AS, Arnett DK, Blaha MJ, Cushman M, Das SR, de Ferranti S, Despres JP, Fullerton HJ, Howard VJ, Huffman MD, Isasi CR, Jimenez MC, Judd SE, Kissela BM, Lichtman JH, Lisabeth LD, Liu S, Mackey RH, Magid DJ, McGuire DK, Mohler ER 3rd, Moy CS, Muntner P, Mussolino ME, Nasir K, Neumar RW, Nichol G, Palaniappan L, Pandey DK, Reeves MJ, Rodriguez CJ, Rosamond W, Sorlie PD, Stein J, Towfighi A, Turan TN, Virani SS, Woo D, Yeh RW, Turner MB. American Heart Association Statistics C, Stroke Statistics S. Heart disease and stroke statistics-2016 update: a report from the American heart association. *Circulation* 2016;**133**:e38–e360.
2. Meier P, Schirmer SH, Lansky AJ, Timmis A, Pitt B, Seiler C. The collateral circulation of the heart. *BMC Med* 2013;**11**:1–7.
3. Seiler C, Stoller M, Pitt B, Meier P. The human coronary collateral circulation: development and clinical importance. *Eur Heart J* 2013;**34**:2674–2682.
4. Tirziu D, Giordano FJ, Simons M. Cell Communications in the Heart. *Circulation* 2010;**122**:928–937.
5. Carmeliet P, Jain RK. Molecular mechanisms and clinical applications of angiogenesis. *Nature* 2011;**473**:298–307.
6. Hsieh PC, Davis ME, Lisowski LK, Lee RT. Endothelial-cardiomyocyte interactions in cardiac development and repair. *Annu Rev Physiol* 2006;**68**:51–66.
7. Tian Y, Morrisey EE. Importance of myocyte-nonmyocyte interactions in cardiac development and disease. *Circ Res* 2012;**110**:1023–1034.
8. Meens MJ, Kwak BR, Duffy HS. Role of connexins and pannexins in cardiovascular physiology. *Cell Mol Life Sci* 2015;**72**:2779–2792.
9. Colombo M, Raposo G, Thery C. Biogenesis, secretion, and intercellular interactions of exosomes and other extracellular vesicles. *Annu Rev Cell Dev Biol* 2014;**30**:255–289.
10. Das S, Halushka MK. Extracellular vesicle microRNA transfer in cardiovascular disease. *Cardiovasc Pathol* 2015;**24**:199–206.
11. Ailawadi S, Wang X, Gu H, Fan GC. Pathologic function and therapeutic potential of exosomes in cardiovascular disease. *Biochim Biophys Acta* 2015;**1852**:1–11.
12. Sahoo S, Klychko E, Thorne T, Misener S, Schultz KM, Millay M, Ito A, Liu T, Kamide C, Agrawal H, Perlman H, Qin G, Kishore R, Losordo DW. Exosomes from human CD34(+) stem cells mediate their proangiogenic paracrine activity. *Circ Res* 2011;**109**:724–728.
13. Vrijsen KR, Sluijter JP, Schuchardt MW, van Balkom BW, Noort WA, Chamuleau SA, Doevendans PA. Cardiomyocyte progenitor cell-derived exosomes stimulate migration of endothelial cells. *J Cell Mol Med* 2010;**14**:1064–1070.
14. Salomon C, Ryan J, Sobrevia L, Kobayashi M, Ashman K, Mitchell M, Rice GE. Exosomal signaling during hypoxia mediates microvascular endothelial cell migration and vasculogenesis. *PLoS One* 2013;**8**:e68451.
15. Bian S, Zhang L, Duan L, Wang X, Min Y, Yu H. Extracellular vesicles derived from human bone marrow mesenchymal stem cells promote angiogenesis in a rat myocardial infarction model. *J Mol Med* 2014;**92**:387–397.
16. Valente M, Araujo A, Esteves T, Laundos TL, Freire AG, Quelhas P, Pinto-do OP, Nascimento DS. Optimized heart sampling and systematic evaluation of cardiac therapies in mouse models of ischemic injury: assessment of cardiac remodeling and semi-automated quantification of myocardial infarct size. *Curr Protoc Mouse Biol* 2015;**5**:359–391.
17. Nascimento DS, Valente M, Esteves T, de Pina Mde F, Guedes JG, Freire A, Quelhas P, Pinto-do OP. MIQuant–semi-automation of infarct size assessment in models of cardiac ischemic injury. *PLoS One* 2011;**6**:e25045.
18. Thery C, Amigorena S, Raposo G, Clayton A. Isolation and characterization of exosomes from cell culture supernatants and biological fluids. *Curr Protoc Cell Biol* 2006;**30:3.22**:3.22.1–3.22.29.
19. Taraboletti G, D'ascenzo S, Borsotti P, Giavazzi R, Pavan A, Dolo V. Shedding of the matrix metalloproteinases MMP-2, MMP-9, and MT1-MMP as membrane vesicle-associated components by endothelial cells. *Am J Pathol* 2002;**160**:673–680.
20. Zhang M, Shah AM. ROS signalling between endothelial cells and cardiac cells. *Cardiovasc Res* 2014;**102**:249–257.
21. Hu GW, Li Q, Niu X, Hu B, Liu J, Zhou SM, Guo SC, Lang HL, Zhang CQ, Wang Y, Deng ZF. Exosomes secreted by human-induced pluripotent stem cell-derived mesenchymal stem cells attenuate limb ischemia by promoting angiogenesis in mice. *Stem Cell Res Ther* 2015;**6**:10.
22. Garcia NA, Ontoria-Oviedo I, Gonzalez-King H, Diez-Juan A, Sepulveda P. Glucose starvation in cardiomyocytes enhances exosome secretion and promotes angiogenesis in endothelial cells. *PLoS One* 2015;**10**:e0138849.
23. Deng L, Blanco FJ, Stevens H, Lu R, Caudrillier A, McBride M, McClure JD, Grant J, Thomas M, Frid M, Stenmark K, White K, Seto AG, Morrell NW, Bradshaw AC, MacLean MR, Baker AH. MicroRNA-143 activation regulates smooth muscle and endothelial cell crosstalk in pulmonary arterial hypertension. *Circ Res* 2015;**117**:870–883.
24. Poliseno L, Tuccoli A, Mariani L, Evangelista M, Citti L, Woods K, Mercatanti A, Hammond S, Rainaldi G. MicroRNAs modulate the angiogenic properties of HUVECs. *Blood* 2006;**108**:3068.
25. Togliatto G, Trombetta A, Dentelli P, Rosso A, Brizzi MF. MIR221/MIR222-driven post-transcriptional regulation of P27KIP1 and P57KIP2 is crucial for high-glucose- and AGE-mediated vascular cell damage. *Diabetologia* 2011;**54**:1930–1940.
26. Yang F, Wang W, Zhou C, Xi W, Yuan L, Chen X, Li Y, Yang A, Zhang J, Wang T. MiR-221/222 promote human glioma cell invasion and angiogenesis by targeting TIMP2. *Tumour Biol* 2015;**36**:3763–3773.

27. Wang M, Ge X, Zheng J, Li D, Liu X, Wang L, Jiang C, Shi Z, Qin L, Liu J, Yang H, Liu L-Z, He J, Zhen L, Jiang B-H. Role and mechanism of miR-222 in arsenic-transformed cells for inducing tumor growth. *Oncotarget* 2016;**7**:17805–17814.
28. Soares AR, Martins-Marques T, Ribeiro-Rodrigues T, Ferreira JV, Catarino S, Pinho MJ, Zuzarte M, Isabel Anjo S, Manadas B, Sluijter JPG, Pereira P, Girao H. Gap junctional protein Cx43 is involved in the communication between extracellular vesicles and mammalian cells. *Sci Rep* 2015;**5**:13243.
29. Barile L, Lionetti V, Cervio E, Matteucci M, Gherghiceanu M, Popescu LM, Torre T, Siclari F, Moccetti T, Vassalli G. Extracellular vesicles from human cardiac progenitor cells inhibit cardiomyocyte apoptosis and improve cardiac function after myocardial infarction. *Cardiovasc Res* 2014;**103**:530–541.
30. Ibrahim AG, Cheng K, Marban E. Exosomes as critical agents of cardiac regeneration triggered by cell therapy. *Stem Cell Rep* 2014;**2**:606–619.
31. Kim H, Cho HJ, Kim SW, Liu B, Choi YJ, Lee J, Sohn YD, Lee MY, Houge MA, Yoon YS. CD31+ cells represent highly angiogenic and vasculogenic cells in bone marrow: novel role of nonendothelial CD31+ cells in neovascularization and their therapeutic effects on ischemic vascular disease. *Circ Res* 2010;**107**:602–614.
32. Contreras A, Orozco AF, Resende M, Schutt RC, Traverse JH, Henry TD, Lai D, Cooke JP, Bolli R, Cohen ML, Moye L, Pepine CJ, Yang PC, Perin EC, Willerson JT, Taylor DA. Identification of cardiovascular risk factors associated with bone marrow cell subsets in patients with STEMI: a biorepository evaluation from the CCTRN TIME and LateTIME clinical trials. *Basic Res Cardiol* 2017;**112**:3.
33. Fernandes T, Baraúna VG, Negrão CE, Phillips MI, Oliveira EM. Aerobic exercise training promotes physiological cardiac remodeling involving a set of microRNAs. *Am J Physiol Heart Circ Physiol* 2015;**309**:H543–H552.